

# Temperature Effect on the Bilayer Stacking in Multilamellar Lipid Vesicles

Joana Valério,<sup>†</sup> M. Helena Lameiro,<sup>†</sup> Sérgio S. Funari,<sup>‡</sup> M. João Moreno,<sup>§</sup> and Eurico Melo<sup>\*,†,||</sup>

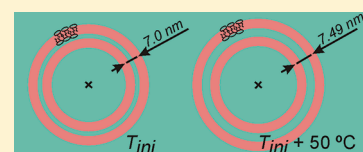
<sup>†</sup>Instituto de Tecnologia Química e Biológica, UNL, Av. da República-EAN, 2780-157 Oeiras, Portugal

<sup>‡</sup>Hasylab, DESY, Notkestrasse 85, D-22607 Hamburg, Germany

<sup>§</sup>Departamento de Química, Universidade de Coimbra, 3004-535 Coimbra, Portugal

<sup>||</sup>Instituto Superior Técnico, Technical University of Lisbon, Av. Rovisco Pais, 1049-001 Lisboa, Portugal

**ABSTRACT:** The small-angle region of the Bragg diffraction of MLV samples is a simple and powerful tool for the study of mesoscopic lipid structures either alone or in interaction with molecules of biological interest. It is also a helpful tool to obtain the much needed thermotropic phase diagrams of lipid mixtures. In the course of our work, we found that the analysis of the diffractograms obtained as a function of temperature is not as straightforward as we expected. When the aqueous medium is concentrated in univalent salts, the small-angle X-ray scattering, SAXS, develops several peaks that have been interpreted to result from regions with different thickness of the interbilayer region. However, a systematic study shows that nonzero ionic strength is by no means a necessary criterion for irregularity of bilayer stacking. We show that MLV in water are uniform and stable if made, kept, and measured at the same temperature. If not, the lamellar repeat distance is smaller than the equilibrated one, eventually developing transient multimodal SAXS diffractions. We present a detailed study of this phenomenon using SAXS and dynamic light scattering and conclude that the deviations from the equilibrium interbilayer distance is a consequence of geometric constraints created by the insufficient thermal expansion of the lipid bilayers.



## INTRODUCTION

Multilamellar vesicles (MLV) are lamellar lipid structures that form spontaneously when water is added to a bilayer-forming lipid. The simplicity of MLV preparation due to their spontaneous formation upon the addition of the aqueous media to the lipid out of the flask makes them the choice for research and pharmaceutical application. When two distinct compartments are needed, separated by a unique stable bilayer, or if for some reason the stacking of several layers is inconvenient, other more specific preparation methods are used. However, multilamellar aggregates are the only choice for techniques that rely on the regular piling up of the bilayers such as in the case of small-angle X-ray powder diffraction analysis (SAXS).

As straightforward as it is, the simple addition of water or buffer to the lipid powder is not always the best choice. Many researchers with the aim of obtaining more reproducible results, namely, to avoid the demixing in the case of mixtures of lipids, use more elaborate methods such as fast injection or freeze-drying that are referred as better suited when the aim is to study thermodynamically equilibrated mixed lipid systems.<sup>1</sup>

If in equilibrium, the average aqueous spacing between bilayers should be regular and controlled by the interplay between attractive van der Waals forces and the joint effect of several repulsive phenomena that range from the enthalpic effects such as the double-layer repulsion, modeled by DLVO theory, and dehydration,<sup>2</sup> or entropically driven steric forces.<sup>3–5</sup> Local distance variation due to undulations, average all over the system and, in practical terms, is reflected in the SAXS experiments by the extended asymmetric lateral wings of the peaks and

is responsible for the difficulty in detecting and characterizing the higher order diffractions,<sup>6,7</sup> specially at temperatures above 50 °C. However, none of the existing models predict the appearance of multimodal peaks.

Researchers that work in the field, especially those that use SAXS in their work, know that, even in the case of pure membrane-forming lipids, the simple scenario presented is only partially corroborated by experiment. It is known that the piling up of the MLV's bilayers is not always as regular as it is generally believed, and multimodal peaks often appear in SAXS that can only have origin in bilayer populations that have different spacing distances. Common reasons for the appearance of populations with different lamellar repeat distance in single lipid membranes can be the nonhomogeneity of the interbilayer aqueous medium that influences the thickness of the aqueous layers, or the deficiently formed MLV where the amount of lipid in adjacent bilayers is not adequate to maintain the equilibrium distances. From our experience, this last reason is not common, only happening sporadically when the protocol of MLV preparation is carefully followed.

A nonhomogeneous interbilayer aqueous medium thickness may arise when the hydration step is done with an aqueous media with a non-negligible concentration of ions giving rise to an uneven distribution of salt concentration. A direct consequence of different ionic concentration in the interbilayer water is the

Received: July 18, 2011

Revised: November 16, 2011

Published: December 12, 2011

change in the equilibrium distance between headgroup interfaces, but a secondary effect is the osmotic differential to which the concentric lamellae are subjected, as proposed by some researchers.<sup>8–10</sup> These authors compared the stacking properties of MLV prepared by hydration of a dry powder and of an even film of lipid obtained by evaporation of the organic solvent in a rotary evaporator, with and without univalent salts added to the aqueous phase, and concluded that the several lamellar stacking distances obtained were a consequence of the different interbilayer concentration of ions. They also proposed a mechanism of hydration that accounts for the hydration-method dependence of the results. Their work was mainly done with POPC and lithium chloride but other lipids and salts were also tested with similar results.

There is no doubt that the ionic strength of the aqueous media with which the hydration is done is important in driving the inhomogeneity of stacking, but the protocol of preparation of MLV can, in principle, also lead to uneven distances. The method of preparation of MLVs has many variants, and each laboratory has its own recipe that determines the time and conditions of the hydration and annealing step, addition of freeze–thaw cycles of the aqueous suspension in an attempt to homogenize the structure or increase the entrapped volume, precleaning of the lipid from eventual contamination by products of lysis, etc. Irrespective of the method used, when the hydration medium is pure water, the dispersion of the lamellar repeat distance of glycerophospholipids measured by SAXS is very small at room temperature, excepting accidental and uncommonly bad samples as already commented.

Samples prepared at room temperature by several methods commonly used in the laboratories for lipid research, when heated at the rate of 1 °C/min develop unexpected multiple diffraction peaks above 40 °C, that make the analysis of the data difficult to interpret if not questionable. The appearance of spurious diffractions is particularly deranging when the objective of the study is to derive the thermotropic properties of lipids or lipid mixtures with the help of SAXS measurements or to study the chemical-physics of membrane interaction. The heating rate of 1 °C/min is often used for analytical methodologies applied to MLV structures such as DSC, FTIR, NMR, or fluorescence but some authors, namely, Sturtevant,<sup>11</sup> recommend speeds as low as 0.2 °C/min. In many cases, namely, when using a synchrotron beamline facility, the time available for the experiments is usually short, and slower heating rates are not practical. It has also to be considered that many samples degrade irreversibly if exposed for long time at high temperatures. It is also obvious that in the absence of a physical explanation of the effect that gives origin to the multimodal diffractions, it is not clear that a smaller rate of temperature change is helpful in eliminating the phenomenon or will eventually mask it. To the best of our knowledge, this difficulty is not documented in the literature and even less is the explanation of its causes and possible workarounds to the problem. In this work, we will focus on the explanation of the physical causes of the appearance of several SAXS peaks at temperatures much different from those of MLV formation under the usual experimental conditions of sample preparation and data acquisition.

To avoid being deceived by the method of MLV preparation, several well-controlled and reproducible techniques of lipid hydration were used. Most of the study was done with DOPC, due to its stable  $L_\alpha$  phase in a convenient temperature range and because it is not suspect of having a microstructure, as it happens

with hybrid lipids such as POPC or OPPC.<sup>12–14</sup> DPPC and POPC were also used to confirm that our observations are not qualitatively dependent on the chemical nature of the lipid acyl chains. All the lipids were previously freed of the always present small contamination of lysis products and the hydration done with pure water.

The multilayered structure of the MLV, particularly the existence of very small internal highly curved vesicles, may be suspect of leading to nonuniformity of bilayer thermal properties. The sequential hydration of the lipid from the outside of the lipid deposit to the inside, result in the initial hydration of the inner layers of the liposome, that can have the consequence of a variation in the water uptake between the internal and external regions of a multilayered liposome and may be responsible for the deviation from ideal stacking. In an attempt to ensure the uniformity of lipid and aqueous systems, we have tested an alternative method for producing multilamellar bilayer assemblies, which is a variant of the reverse phase evaporation technique, REV. Reverse phase evaporation with emulsion inversion is often used when large unilamellar vesicles, LUV, are desired, but it may also produce multilamellar systems if the ratio of lipid to water is large.<sup>15,16</sup> It is claimed that the multilamellar systems created in this way are large and that the inner lamellae are adjacent to the outer one without the imbedded small structures as in the case of spontaneous MLV. This should result in vesicles with evenly distributed solutes that do not show the anomalies of the MLV.

## MATERIALS AND METHODS

**Reagents.** The phospholipids 1,2-dioleoyl-*sn*-glycero-3-phosphocholine (DOPC), 1-palmitoyl-2-oleoyl-*sn*-glycero-3-phosphocholine (POPC), and 1,2-dipalmitoyl-*sn*-glycero-3-phosphocholine (DPPC) were obtained from Avanti Polar Lipids. Chloroform was from Lab-Scan, HPLC grade, and NaCl Riedel de Haën, p.a. grade. Benzene (Lab-Scan, HPLC grade) and methanol (Merck, LiChrosolv) were dried with anhydrous magnesium sulfate (Riedel-de-Haën) before use.

Ethyl ether (Lab-Scan, HPLC grade) was freed from peroxides by passing through a column containing aluminum oxide as recommended by Dasler and Bauer<sup>17</sup> and regularly checked for peroxide buildup using the potassium iodide test.

Water was double distilled and further purified with an Elgastat UHQ-PS system. All the water for lipid hydration was 0.05 mM in EDTA.

**Lipid Purification.** All phospholipids, even when kept under Argon at –20 °C, have a residual amount of lysed lipid that may not be detected with the usual TLC test but is revealed by the appearance of foam when hydrated. To clean the phospholipids, we prepared MLV by the standard film method and submitted the suspension to several cycles consisting of freeze–thaw, followed by centrifugation and resuspension of the pellet in pure water, that were repeated until no more foam is observed. Excess water from the last pellet was removed by vacuum ( $10^{-2}$  mmHg, 2 h at room temperature). The dry precipitate dissolved in benzene was evaporated to remove the remaining water by azeotrope distillation. Lastly, the lipid was freeze-dried from benzene, the powder kept in an inert atmosphere at –20 °C, and used within one month. All manipulations of unsaturated lipids in this and subsequent preparations were done under nitrogen or argon.

**Preparation of MLV.** Since one of our concerns is the uniformity of hydration of the lipid forming the multilayered

structures, we tested several variants of the conventional MLV preparation technique.<sup>18</sup> The starting state of the lipid before hydration was either a film obtained from solvent ( $\text{CHCl}_3$ ) removal in a rotary evaporator or the powder formed by freeze-drying from benzene. In both cases, two hydration protocols were tested that are here named fast and slow hydration. In the fast hydration method, the aqueous media is directly added to the lipid at a temperature above the lipid main phase transition without a previous exposure to a humid atmosphere. The slow hydration was identical to the fast except that the addition of aqueous phase was done after keeping the lipid, powder, or film for 24 h in 98% humidity, also above the main phase transition temperature of the lipid. In an attempt to reorganize the lamellar arrangement, some samples were subjected to freeze–thaw cycles followed by slow annealing. Because of the possible accidental inconsistency in the preparation, at least two independent samples were made with each method.

As an alternative to hydration with water, we also used 100 and 500 mM NaCl.

When we wanted to maintain the samples at the same temperature from hydration until measurement, the freeze-dried lipid powder was transferred to a vial and the aqueous media added at the required temperature. The temperature was maintained along all manipulations, including overnight hydration, centrifugation, transfer to the capillary, and subsequent centrifugation and closing. The sample was stabilized for 2 days at the same temperature and directly transferred to the preheated sample-holder.

**Preparation of MLV-REVs.** Multilayered REV vesicles were prepared using the method developed by Pidgeon et al., that is based on the reverse phase evaporation technique for formation of large unilamellar vesicles, in which the ratio between the mass of lipid and water is increased by ca.  $10\times$ .<sup>15,16</sup> For X-ray samples, 100 mg of lipid was dissolved in 2 mL of diethyl ether into which 60  $\mu\text{L}$  of aqueous media was rapidly injected. The sample was sonicated under argon for 2 min at 25  $^\circ\text{C}$ , and the ether evaporated in a rotary evaporator at 37  $^\circ\text{C}$  and 700 mmHg until formation of a semisolid gel. The gel was vigorously agitated in a vortex to induce emulsion inversion, easily noticed by the change of the fluidity of the suspension, and the remaining organic solvent removed in the rotary evaporator at 37  $^\circ\text{C}$  and 450 mmHg. To eliminate small lipid aggregates that may be present, the preparations were washed twice with the aqueous media and centrifuged at 10 000g for 10 min. The residual ether was removed by overnight dialysis against the aqueous media saturated with nitrogen.

**Preparation of Extrusion LUV (LUVET).** Large unilamellar vesicles, LUV, of DOPC and POPC were prepared by repetitive extrusion of a MLV suspension in water (1.25, 2.5, or 5 mM in lipid) with high  $\text{N}_2$  pressure through 100 nm pore Nuclepore polycarbonate filters (Corning, Acton, MA, USA) at room temperature according to a well-known methodology.<sup>19,20</sup> The final suspension was centrifuged for 10 min at 1 kg to free the solution of the more dense particles.

**X-ray Diffraction.** Small angle X-ray scattering data was collected at the synchrotron radiation facility beamline A2 of the Soft Condensed Matter laboratory at the storage ring DORIS III of the Deutsches Elektronen Synchrotron (DESY), using a setup previously described.<sup>21</sup> The samples in capillary tubes were prepared as follows: the vesicle suspension is previously centrifuged at 30 kg for 10 min and the pellet with a small amount of aqueous medium transferred to the capillary tube (1.0 mm

diameter with 0.01 mm wall glass, Markröhrchen, Germany). Capillaries were centrifuged for 10 min at 1250g and, before being closed, left 24 h under an argon atmosphere saturated with water to avoid possible oxidation processes before and during X-ray irradiation.

The measurements were done with the capillary in a temperature-controlled holder first slowly cooled from room temperature until 4  $^\circ\text{C}$  and then heated until 86 at 1.0  $^\circ\text{C}/\text{min}$ , maintained at 86  $^\circ\text{C}$  for 4 min, to check for sample structural stability, and subsequently returned to 20  $^\circ\text{C}$ . Data acquisition lasted for 20 s every 120 s (corresponding to ca. 2  $^\circ\text{C}$ ). The real temperature of the sample holder at the beginning of each data collection was registered together with the corresponding CCD image. For some samples, the heating was stopped at selected temperatures and kept at this temperature for 60 min with measurement every 2 min.

The SAXS region was calibrated with rat tail collagen, and the marCCD output linearized with an in-house developed program (A2tool, A. Rothkirch, Hasylab, DESY). The distance to the beam center of the observed diffraction rings was converted into reciprocal spacing,  $s = 1/d$ , where  $d$  is the distance between the diffracting planes. A second calibration with rat tail collagen after a set of experiments confirmed the stability of the instrumental setup.

The background noise profile obtained from a long data acquisition (30  $\times$  20 s) of a capillary filled with water was subtracted from the experimental diffractograms. The evaluated error in  $s$  in the SAXS region considered is of 0.001  $\text{nm}^{-1}$ . To characterize multimodal SAXS Bragg peaks, we opted to fit the data to a linear combination of Lorentzian functions using the package Origin 7 (OriginLab Co., Northampton, USA). Since a single Lorentzian is known to be quite adequate to describe the single-component diffractions, the use of other more sophisticated model equations did not add further understanding to the aspects we intend to prove.

**Dynamic Light Scattering.** Data was acquired with a Malvern Nano ZS (Malvern Instruments, Malvern, UK). To simulate as close as possible the experimental thermal conditions used in the X-ray experiments, the samples in 1 cm silica cuvettes were heated in steps of 2  $^\circ\text{C}$ , followed by a 2 min equilibration, and two measurements were averaged at each temperature resulting in a total time for a heating run of approximately 90 and 120 min for cooling, times that include the thermal equilibration and the duration of measurements. The LUVET experiments gave clean correlation functions and a single peak with an average polydispersity index of ca. 0.075. For lipid concentrations at and below 2.5 mM, identical results are obtained, and we opted to make all measurements with 1.25 mM samples. Identical experiments were tried with LUV prepared by reverse phase evaporation<sup>22</sup> but were not conclusive due to the polydispersity of size.

We also questioned what should be the effect on the experimentally determined hydrodynamic radius,  $R_H$ , of a liposome that changes shape from spherical to a prolate spheroid with axial ratio  $p = a/b$ , where  $a$  and  $b$  are, respectively, the axial and equatorial semiaxes. The Perrin factor,  $F = f_H/f_S = R_H/R_S$ , relates the frictional coefficient of a diffusing object,  $f_H$ , to that of an equivalent sphere,  $f_S$ . For a prolate spheroid,  $F$  can be calculated from  $p$  using the expression<sup>23</sup>

$$F = \frac{\sqrt{p^2 - 1}}{\sqrt{p} \ln \left( p + \sqrt{p^2 - 1} \right)} \quad (1)$$



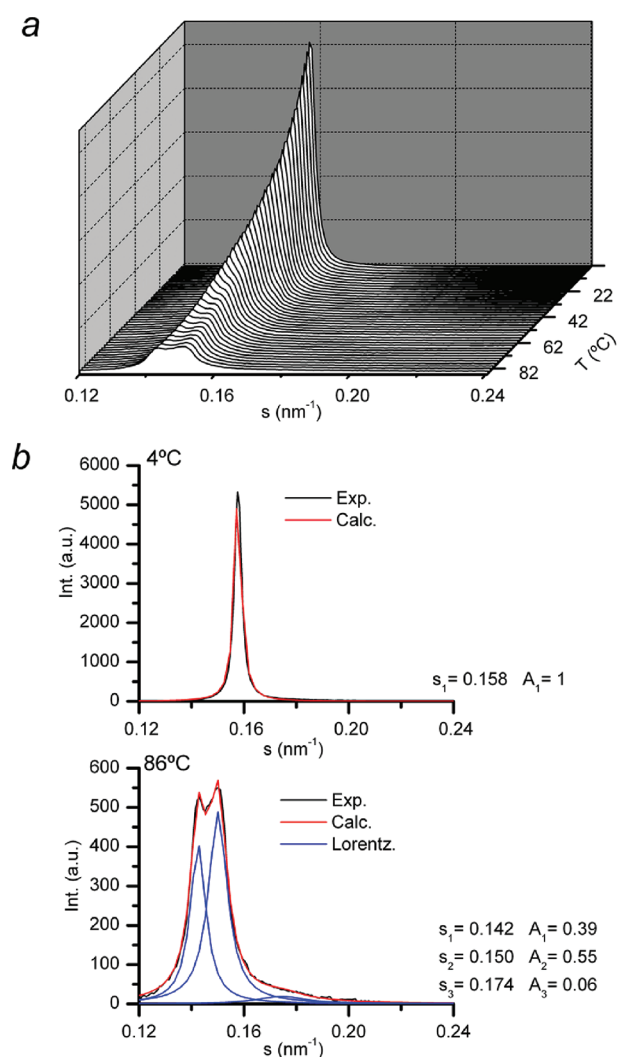


**Figure 1.** Panel a, the thermal evolution of the sample of DOPC MLV shows the formation of two main peaks and a shoulder at lower scattering vector values, that begin to be visible at ca. 40 °C. The shoulder eventually originates the long tail described by a Lorentzian at 0.174 nm<sup>-1</sup> at 86 °C, panel b. From 4 to 40 °C, the diffraction fits to a single Lorentzian as shown for 4 °C in panel b, but when increasing the temperature at the rate of 1 °C/min, at least 2 or 3 components are needed as presented in panel b for 86 °C.

The determination of  $R_S$  from the molar mass,  $M_w$ , and specific volume,  $\bar{V}$ , of the lipid, considering a monodisperse system, is straightforward,  $R_S = (3M_w\bar{V}/4\pi N_A)^{1/3}$ . In the calculation, we considered the thickness of the solvent layer equal to 0.24 nm and the thickness of the bilayer as 4.6 nm.

## RESULTS AND DISCUSSION

**SAXS of MLV and MLV-REV in Water.** X-ray diffractograms in the small-angle region of MLV suspensions in water do not always conform to what is expected from regularly stacked systems. Not considering accidental situations where the irregular stacking may be ascribed to a bad sample preparation, it is common to observe a departure from the ideal behavior once the temperature is increased by a few tens of degrees above that at which the system was prepared and/or kept before measurement. In Figure 1, we show the typical thermal evolution of the

first order SAXS peak of a sample of MLV of DOPC in water made by the technique that we name as film/slow in the Materials and Methods section when heated from 4 to 86 °C at a 1 °C/min rate, together with the decomposition in Lorentzians at 4 and 86 °C.

In the diffractogram of Figure 1, panel a, the appearance of a shoulder at a lower reciprocal distance is noticeable above ca. 40 °C that eventually develops into a strong peak at higher temperatures. While until 40 °C a single Lorentzian fits the diffraction peak, having a maximum at  $s = 0.158$  nm<sup>-1</sup> at 4 °C with full width at half-maximum (fwhm) of 0.004 nm<sup>-1</sup>, at 86 °C at least three components at  $s = 0.142$ , 0.150, and 0.174 nm<sup>-1</sup> are needed to describe the diffraction, panel b. In this and following diffractograms, the broadening of the diffraction for high temperatures is to be expected,<sup>24</sup> namely, the peak should not have a Lorentzian shape. Here, we are not concerned with the fit of a theoretical model to the experimental data but with the presence of shoulders and multiple peaks that are not accounted for by the existing models.

An identically prepared sample subjected to freeze–thaw after MLV formation results in a marginally thinner stacking distance at 4 °C located at 0.159 nm<sup>-1</sup>. However, increasing the temperature, the behavior does not differ from what was observed with the non freeze–thawed sample except for an improvement in the sharpness of the peaks demonstrating a better spatial correlation. As with the non freeze–thawed sample, to obtain a reasonable description of the SAXS first order diffractogram at 86 °C, three Lorentzians are needed, with peaks at  $s = 0.146$ , 0.152, and 0.169 nm<sup>-1</sup>; see Table 1.

Samples done with fast film hydration or freeze-dried powder followed by fast or slow hydration do not result in patterns qualitatively different from the one presented in Figure 1. All samples show nonuniform bilayer assembling above 40 °C. Fast hydration of the powder presents an apparent better uniformity needing only two Lorentzians at  $s = 0.142$  and 0.153 nm<sup>-1</sup> to fit the diffractogram at 86 °C (Table 1), but this is probably due to a poorer stacking revealed by the larger peaks that fit the data, which are twice as wide as those from the other methods and/or less dense samples that cause a less favorable signal-to-noise ratio in the SAXS.

The thermal evolution of the reciprocal spacing,  $s$ , of what we could call the base component of the diffraction follows the expected trend with temperature:<sup>7,25,26</sup> it slowly increases from 4 to ca. 40 °C due to the increase in the aqueous layer thickness that is partially compensated by the bilayer thinning caused by chain conformational disorder, and for higher temperatures, it systematically decreases due to the increase of the interbilayer repulsive forces. We do not necessarily identify this base component with the stronger peak, as will be later discussed. If a common pattern is to be drawn from the generality of the data obtained with the several preparation conditions and a sample heating rate of 1 °C/min, we would say that a single component is present from 4 to ca. 40 °C, temperature above which one or more shoulders begin to appear at larger and smaller reciprocal distances that for higher temperatures develop in a clear multimodal diffraction. At 86 °C, the strong diffraction consists of the overlap of two components with variable but similar relative intensity separated by ca. 0.01 nm<sup>-1</sup> accompanied by a third broad smaller band, in several cases prominent, with a maximum in the region of 0.16–0.17 nm<sup>-1</sup>. The question may be raised whether this last peak is not a fitting expedient that accounts for the peak asymmetry predicted by the Caillé model.<sup>7,27–29</sup>

**Table 1.** Data Obtained from the Lorentzian Decomposition of SAXS Signals at Low and High Temperature for the Lipids Tested and Several Aqueous Media and Method of Preparation Characteristics

sample	preparation method	<i>T</i> (°C)	<i>s</i> (nm <sup>-1</sup> )/normalized integrated intensity from Lorentzian decomposition
DOPC water	MLV	4	0.158/1.00
		86	0.142/0.39
			0.150/0.55
			0.174/0.06
	film	4	0.158/1.00
		86	0.151/0.50
			0.156/0.30
			0.158/0.20
	slow hydration	4	0.159/1.00
		86	0.146/0.49
			0.153/0.39
			0.169/0.11
	f-t	4	0.156/1.00
		86	0.142/0.49
			0.153/0.51
			0.152/1.00
	MLV-REV	86	0.145/0.14
			0.150/0.37
			0.205/0.49
			0.157/1.00
POPC water	MLV	20	0.157/1.00
		40	0.151/1.00
		55	0.149/1.00
		70	0.145/1.00
	film	85	0.144/1.00
			0.135/0.19
DPPC water	fast hydration		0.149/0.55
			0.166/0.26
	f-t		0.146/1.00 (bad fit)
			0.144/0.22
DPPC water	slow hydration		0.146/0.24
			0.149/0.56

<sup>a</sup> Hydrated and measured at the same temperature.

Depending on the sample, this band is more or less pronounced, but even for the best samples (freeze-dried fast hydration), its shape is not that of a long tail as the one that can be simulated using the second order approximation of the Caillé's structure factor according to eqs 19, 24, and 28 of Gordeliy et al.<sup>7</sup>

The experiments were repeated with other glycerophosphocholines, POPC, and DPPC, and in all cases, the behavior is similar to that of DOPC; see Table 1.

The possible interference of impurities, namely, fatty acid and lyso-PC, that can be present due to the time elapsed between preparation and measurement was ruled out by measuring samples of POPC MLV to which lyso-PPC and oleic acid were added simulating 5 and 10 mol % POPC lysis. At 4 °C, the Bragg peak is broader in the presence of the impurities, but a single diffraction is detected with the maximum shifted by 0.008 and 0.012 nm<sup>-1</sup> to smaller reciprocal distance, respectively, for the

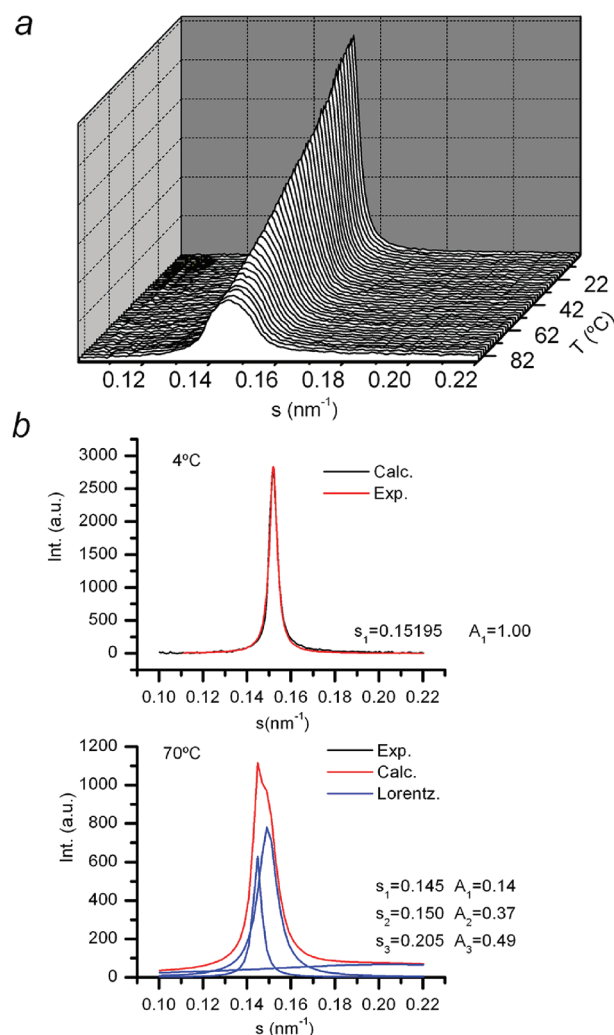


**Figure 2.** Evolution of the 1st order peak of the SAXS with the temperature, increased at a rate of 1 °C/min, of a sample of MLV-REV of DOPC in water. In the 3D representation, panel a, no clear shoulders at high temperature are observed similar to those seen in Figure 1, due to the broadness of the peak indicating an inferior spatial correlation. However, above 40 °C, the two Lorentzians corresponding to two visually evident peaks are needed for the fit, as shown for 70 °C in panel b.

5 and 10 mol % case, probably due to the repulsion of the charged fatty acid headgroups. However, the SAXS multiple peaks that develop at high temperature are neither more pronounced nor differing in relevant aspects from those observed with pure POPC, data not shown, and we conclude that lysis cannot be responsible for the appearance of new peaks.

From these experiments, we can conclude that with the increase of temperature at the rate of 1 °C/min, a nonuniformity of stacking is developed above ca. 40 °C independent of the method of hydration and diacyl-glycerophosphocholine used. Given that the MLV contain internal sub-MLV, forming a multionion-like structure, where the internal layers have a much higher curvature than the external ones, one possible explanation may reside in a different reaction of the two regions to the temperature.

To check for the possible effect of internal smaller MLV, we prepared MLV-REV in water that are described as having a

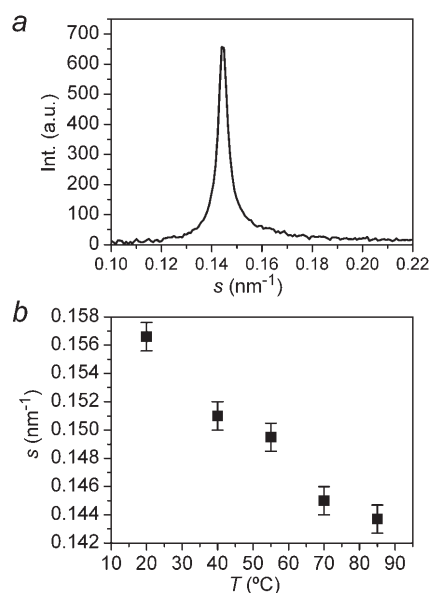


**Figure 3.** First order SAXS peak of samples prepared, maintained, and measured at the same temperature as described in the Materials and Methods section. In panel a, for 70 °C, the peak is unimodal in contrast to what is observed with those samples prepared and kept at room temperature until measurement. The same happens for 40, 55, and 85 °C. In panel b, the reciprocal distances obtained with samples prepared and kept at the measurement temperature are plotted as a function of  $T$ .

multilayer stacking only adjacent to the external bilayer.<sup>15,16</sup> The SAXS profile, shown in Figure 2, is similar to that obtained with the fast hydration of the freeze-dried sample. However, the lamellar repeat distance is somewhat larger,  $s = 0.152$  nm<sup>-1</sup>, at 4 °C; the fwhm of the first order peak is equally small,  $0.004$  nm<sup>-1</sup>, but, despite some nonreproducibility of the method, most samples give good single Lorentzian fits up to 40 °C. Above this temperature, at least two Lorentzians are needed in order to describe the diffractogram:  $s = 0.145$  and  $0.150$  nm<sup>-1</sup> together with a very long tail at 86 °C. Being much noisier than the diffraction pattern of the other MLV used in this work, it is risky to affirm that no other peaks are present either at lower or higher  $s$  values, though, they do not appear on visual inspection of the 3D plots.

From the experiments with MLV-REV, we conclude that the phenomenon observed is not related with the highly curved inner bilayers present in the common MLV. The nonuniform bilayer stacking and the weaker signal of the MLV-REV make the observation less obvious, but the effect is present and not qualitatively different from what is seen with conventional MLV.

From the above, two questions are left open: (i) are these observations attributable to the difference in the temperature at which the samples were prepared and stored, or are they intrinsic to these bilayers at high temperature, and (ii) was the heating rate of  $1$  °C/min too fast for the equilibration of the system? One experiment that can clarify the first point would be to prepare and maintain the MLV at a stable high temperature beginning with preparation and ending with measurement. Because the procedure is not experimentally straightforward, we used several samples for each temperature 40, 55, 70, and 85 °C. In all experiments, a sharp and unimodal first order peak is systematically obtained, similar to what is observed at 20 °C with samples prepared at room temperature. Therefore, the complex

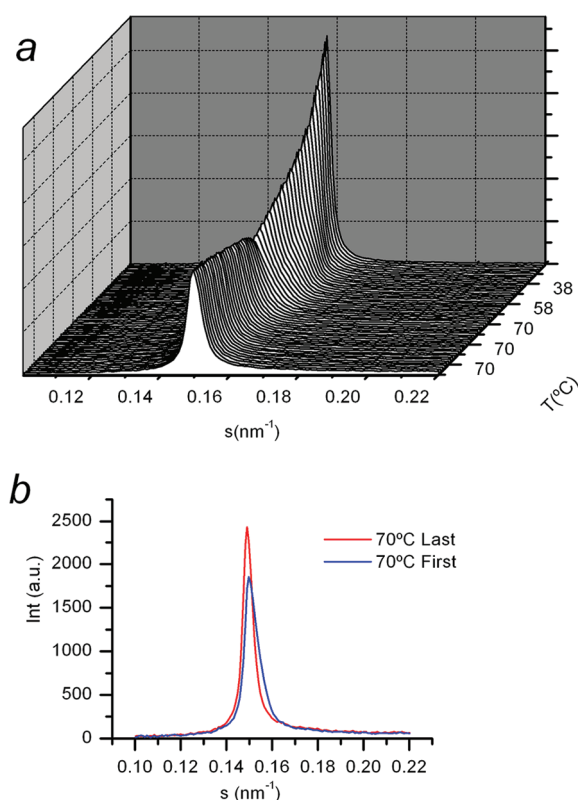


**Figure 4.** Diffractogram of the sample heated from 20 to 70 °C and maintained at this temperature for 1 h, panel a. In panel b, the first and last measurement of the first order peak at 70 °C.

diffractions have origin in the difference between the preparation and measurement temperatures. In Figure 3a, we show the first order peak with maximum at  $s = 0.145$  nm<sup>-1</sup> and fwhm =  $0.005$  nm<sup>-1</sup> for 70 °C, a temperature at which the multimodal diffractions are already conspicuous. The reciprocal distances obtained for all the temperatures studied by this method are presented in panel b of the same figure.

To find out if the temperature scan rate is too high, samples were heated at a rate of  $1$  °C/min from 20 until 70 °C and then kept and measured every 2 min for 1 h at 70 °C, Figure 4. The sample is prepared by the freeze-dry method with fast hydration at room temperature, and the clear shoulder at high  $s$  observed in the first diffractograms at 70 °C disappears in favor of a sharp first order peak at  $s = 0.149$  nm<sup>-1</sup> with fwhm =  $0.005$  nm<sup>-1</sup>; see Figure 4. This rearrangement takes ca. 40 min, after which time the peak is unimodal and apparently stable. The behavior is similar for a sample heated from 20 to 40 °C and left at this temperature for 1 h. In this case, the peak is always clean of shoulders but becomes sharper and has a small shift from  $0.155$  to  $0.154$  nm<sup>-1</sup> that also takes about 40 min to complete; data not shown. From these experiments, we conclude that the rate of temperature change is then responsible for the appearance of several peaks at high temperature, but it is clear that the spacing attained after one hour at 40 or 70 °C is not the same that is observed for the sample kept at the same temperature from hydration until measurement; see Table 1.

Comparing Figures 3a and 4, while both, the sample made at 70 °C and that heated and left to stabilize, have a sharp peak, fwhm =  $0.005$  nm<sup>-1</sup>, they differ in their layer spacing by an amount that largely exceeds the experimental uncertainty; the



first having a repeat distance of 6.90 nm, while that of the sample left to stabilize in the sample holder only attains 6.71 nm. This difference could result from lysis of the lipid along the 2 days it was maintained at 70 °C before measurement, but this hypothesis was discarded by TLC analysis of the capillary content. Additionally, the presence of the lysis products should also be reflected in the width of the peaks that is not observed.

The difference in the repeat distance at 70 °C in these two experiments can only be interpreted as an inability of the sample prepared at room temperature to attain the equilibrium spacing at this temperature. Identical conclusion can be extracted from the 40 °C experiments.

To summarize, it can be said that until about 40 °C, the behavior of the X-ray diffraction of samples prepared at room temperature is apparently normal, an appearance that is challenged by the observation that the diffraction shifts to lower  $s$  values if the sample is left at 40 °C for 1 h. Above 40 °C, the birth of new peaks is observed at lower and higher reciprocal distances, not visible in the perspectives used in the above figures, peaks that eventually disappear, indicating a complex process in the rearrangement of the several MLV sampled by the X-ray beam. However, if the samples are allowed to stand for time enough at the measuring temperature, a pseudoequilibrium is attained, that differs from the real equilibrium in having a smaller repetition distance. This process is slow; the time needed for attaining the pseudoequilibrium for a sample heated from 20 to 70 °C being close to 2 h, what would only be possible with a heating rate much slower than 1 °C/min.

From what exists in the literature, it is not clear why the MLV system has such difficulty in attaining a new equilibrium state. The kinetics of lipid reorganization of MLV in the vicinity of lipid structural transitions after a temperature jump of a few K has been thoroughly investigated,<sup>30,31</sup> and the time taken for the system to stabilize is in the sub-10 s range, so it seems that a process with an expected smaller activation energy would be faster to complete. The repeat distance of the MLV bilayers is a function of the bilayer head to head and interbilayer water thickness, both temperature-dependent,<sup>25,26</sup> but also of the constraints imposed by the thermal expansion of the concentric vesicles, a trivial geometric effect that, to the best of our knowledge, has never been considered. The thermal area expansion of the bilayer and the reduction of the headgroup to headgroup bilayer thickness are well documented in the literature,<sup>25,32,33</sup> the same applying to the thermodynamics of the bilayer–bilayer interactions that has been the subject of extensive discussion and theoretical refinement along the past decades.<sup>4,7,26,28</sup> However, an aspect that has been neglected is the geometrical consequence for the topology of the MLV of bilayer thinning and lateral expansion with temperature. In other words, the interbilayer spacing is geometrically forced by the thermal area expansion of the individual layers of a MLV, and the resulting spacing may or not be the one desirable to maintain the bilayer–bilayer interaction at its equilibrium distance. As we will show, to attain equilibrium, the lipid should exchange between adjacent bilayers, a process that for long-chain phospholipids is too slow<sup>34,35</sup> to be of practical interest in the lifetime of a sample, not to mention the time-scale of a measurement. The consequence of this thermal area growth for the topology adopted by the bilayers in a MLV is not negligible, as we will discuss in the next paragraphs.

Before trying a detailed explanation of the evolution of the experimentally observed repeat distance with temperature, we will concentrate on exploring the consequences of the thermal

expansion of the individual vesicles constituting a MLV. The studies of bilayer water permeation are quite consistent in that water crosses the phospholipid bilayer in subseconds to seconds,<sup>36,37</sup> that is 2 orders of magnitude faster than the time scale of the X-ray experiments described. It is useful to understand first what would happen to a vesicle with an impermeable membrane when the temperature is changed. When subjected to a temperature increase from an arbitrary  $T_{\text{ini}}$  until  $T_{\text{ini}} + 50$  °C, the area of the bilayer will expand, and if no water is allowed to cross the membrane, the expansion of the internal water has also to be taken into account. For the present purpose, we may consider that the coefficient of volumetric thermal expansion,  $\alpha$ , of water as constant and equal to that at 30 °C ( $\alpha = 3.8 \times 10^{-4} \text{ K}^{-1}$ ) in the 50 °C temperature range of our simulation and that for the area thermal expansion,  $\sigma$ , of DOPC bilayers is also constant and equal to the published value for the same temperature ( $\sigma = 2.9 \times 10^{-3} \text{ K}^{-1}$ ).<sup>26,33,38</sup> Under these conditions, the volume of the water included in a liposome with a radius of 1000 nm heated from  $T_{\text{ini}}$  until  $T_{\text{ini}} + 50$  °C will grow by  $7.9 \times 10^7 \text{ nm}^3$ , but the growth of the area of the lipid bilayer will impose an increase in its internal volume of  $9.7 \times 10^8 \text{ nm}^3$  if the spherical shape is maintained. Therefore, the vesicle must assume a shape compatible with a larger specific surface to fit the small water volume filling its internal space. Any nonspherical shape could satisfy the new geometrical constraints. One possibility is the formation of a prolate spheroid (with axes  $a = b < c$ ) that, to comply with the relationship between volume and surface area, will need to adopt an axial ratio  $c/a = 2.6$ , geometrically quite far from the original sphere. Generalizing, if the bilayer is impermeable to the water, when the temperature changes from that at which the vesicle was created to a higher temperature, the vesicle will have to change from whatever shape it originally had, in principle, spherical, to a new one with a larger specific surface. What is to be retained from this simulation is the remarkable shape perturbation resulting from the temperature change that may not be 100% recovered in a continuous 1 °C/min heating of a multilayer system.

If enough time for equilibrating the inner and outer water is given, no constraints will be created by the independent expansion of the encapsulated water, and only the expansion of the vesicle wall has to be taken into account. To keep the calculation simple, we consider only what happens to two concentric spherical vesicles in the  $L_\alpha$  phase with a bilayer thickness of 4.6 nm, the external vesicle with radius  $R = 1000$  nm, and the internal with  $R = 993$  nm forming a bilamellar vesicle as schematically shown in Figure 5. The thickness of the spherical shell separating the two spheres,  $\Delta R$ , at any given temperature,  $T$ , is a function of its separation at the initial temperature  $T_{\text{ini}}$ , and of the area thermal expansion,  $\sigma$ . If  $\sigma$  is considered constant, we obtain the relationship

$$\Delta R_T = \sqrt{1 + \sigma(T - T_{\text{ini}})} \Delta R_{T_{\text{ini}}}$$

For the thermal area expansion given above and for an initial separation,  $\Delta R_{T_{\text{ini}}} = 7.0$  nm, the thickness of the spherical shell at  $T = T_{\text{ini}} + 50$  °C is  $\Delta R_T = 7.49$  nm. In the conditions of this simulation, the system will only be at equilibrium if the combined decrease of the bilayer thickness,  $d_B - d_{B_{\text{ini}}}$ , together with the increase of the width of the aqueous interbilayer region,  $d_W - d_{W_{\text{ini}}}$ , due to the 50 °C temperature increase, equals +0.49 nm. This spacing will only, by chance, be the value interbilayer forces

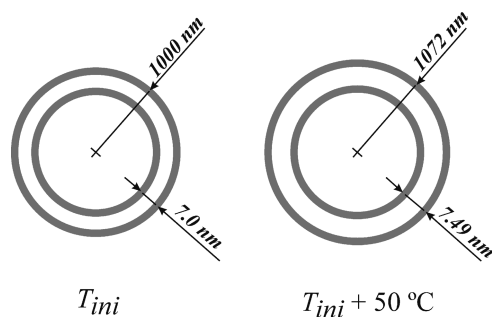


**Figure 5.** Schematic representation (not drawn to scale) of the effect of the increase of 50 °C on the geometry of DOPC spherical vesicles considering negligible the exchange of lipid between bilayers freely permeable to water. The initial bilamellar vesicle at a temperature  $T_{ini}$  is heated until  $T_{ini} + 50$  °C supposing the thermal expansion coefficients of the lipid to be constant. The spherical shape and even distance may be maintained, but the interbilayer distance is determined by geometrical factors rather than by the thermodynamic equilibrium distance.

impose, and to restore the equilibrium, phospholipid has to migrate between bilayers, a process that is known to be very slow.

The experiments done at constant temperature from hydration to measurement result in equilibrated samples that allowed the determination of the MLV equilibrium lamellar repeat distance; see Figure 3b. The distances obtained for 20 and 40 °C,  $\Delta R = 6.39$  and 6.62 nm, respectively, are compatible with a thermal area expansivity  $\sigma = 3.7 \times 10^{-3} \text{ K}^{-1}$ , which is about 30% higher than the literature value for 30 °C. Therefore, if the published  $\sigma = 2.9 \times 10^{-3} \text{ K}^{-1}$  is accepted as correct, when heating the MLV suspension, the bilayers are not allowed to thermally expand as much as required for the equilibrium distance to be attained, and the system is forced to accommodate at smaller than equilibrium distances. The experimental observation that at higher temperatures several peaks and a long tail develop for larger  $s$  values (smaller distances) is certainly a consequence of this constriction.

It should be commented that the thermal expansion for DOPC given by Evans and Needham,<sup>38</sup>  $3 \times 10^{-3} \text{ K}^{-1}$ , was proposed more as a guiding number than as an exact experimental parameter, and the more recent determination by Pan et al.,<sup>26</sup> giving a virtually identical value at 30 °C,  $2.9 \times 10^{-3} \text{ K}^{-1}$ , was obtained for lipids layered on a silicon substrate. In our experiments, this value may differ not only due to the range of temperatures used but also because the bilayers are not planar.

A direct measurement of the extent of the perturbation of vesicle dimension and shape due to the increase of temperature may be obtained by determining the change in hydrodynamic radius with the temperature of a monodisperse population of large unilamellar vesicles using dynamic light scattering.

**DLS of LUVET in Water.** We have prepared extrusion LUV of DOPC in water as described in the Materials and Methods section and studied the DLS of the suspensions obtained as a function of temperature. The LUVET are quite monodispersed as expected<sup>39,40</sup> with an average hydrodynamic radius,  $R_H$ , of 46.2 nm at 20 °C corresponding to a slightly smaller diameter than the filter holes (100 nm) in accordance with what is reported by several authors.<sup>20,40</sup> The samples were heated from 20 °C until 70 °C and subsequently cooled back to 20 °C, and data was obtained every 2 °C in both directions. The timing of the sequence of measurements reproduces fairly well the conditions used in X-ray experiments (details in the Materials and Methods section).

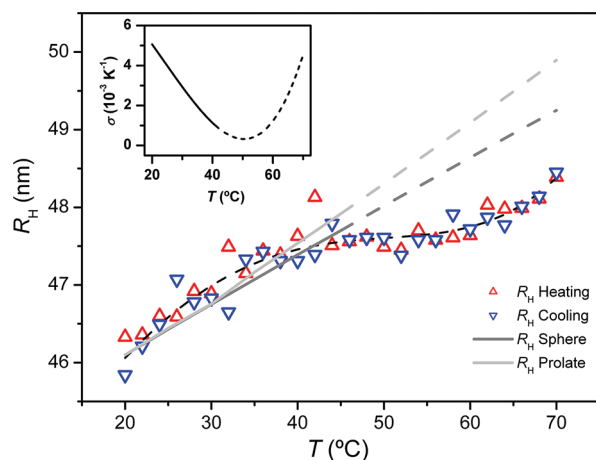


**Figure 6.** Dependence of the hydrodynamic radius of extrusion unilamellar liposomes on temperature obtained by DLS for the heating (red triangle) and cooling (blue triangle) runs. The dotted line accompanying the experimental points is not derived from a model and is only included as a guide to the eye. The  $R_H$  for a sphere (—) and for a prolate spheroid (---) were calculated as explained in the text. The inset shows the thermal area expansion,  $\sigma$ , of the bilayer, calculated from the experimental  $R_H$  temperature dependence.

The hydrodynamic radii,  $R_H$ , obtained as a function of temperature are represented in Figure 6 (the dashed line accompanying the experimental points is only a guide to the eye). A simple inspection of the heating and cooling data shows that, in the time-scale of the experiment, the LUVET maintain their properties unchanged. In the same figure, we represent the expected increase of  $R_H$  based on the hypothetical spherical shape of the vesicles at 20 °C (black solid line) where the hydrodynamic radius is calculated accounting only for the area dilation of the DOPC bilayer given above,  $\sigma = 2.9 \times 10^{-3} \text{ K}^{-1}$ . The calculation was done supposing that the spherical shape is maintained, what amounts to say that the bilayer is infinitely permeable to water in the time scale of the experiment and that when the vesicles swell, they continue to have a spherical shape. With small deviations, the hydrodynamic radius follows remarkably well the prediction of the model based only on bilayer thermal expansion until ca. 40 °C. If we question what would happen if the bilayer were not permeable to water, the answer is in the gray curve for the diffusion of the prolate spheroid that is the more plausible shape change since an oblate shape results in a smaller  $R_H$ . The difference in diffusion between the two shapes is not large in this temperature range, and both are in accordance with the experimental data. The inset of Figure 6 shows the dependence of temperature of the DOPC thermal area expansion calculated from the experimental data using the definition,  $\sigma = (dA/dT)/A$ . It is comfortable to see that the value obtained for  $\sigma$  at 30 °C is  $2.9 \times 10^{-3} \text{ K}^{-1}$ , coincident within the experimental error, with the published value for the same temperature. What is surprising is the strong variation of  $\sigma$  in the region from 20 to 40 °C. The in-plane thermal expansion of a fluid bilayer results from three partially independent factors: the usual effect of the anharmonicity of the intermolecular potential energy curve common to all molecular solids and liquids, the increase in the free volume characteristic of liquids, and additionally the progressive increase of the number of the gauche configurations along the hydrocarbon chains. All these phenomena contribute to the area expansion of a bilayer, but only the last one plays a role in the



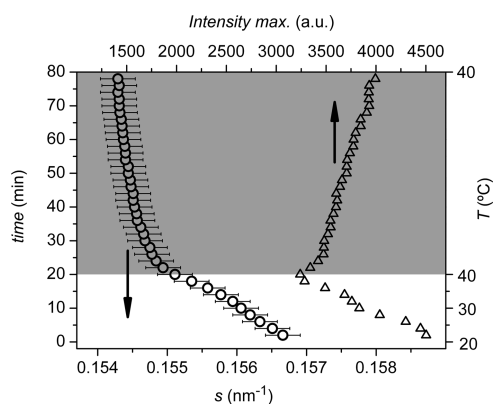


**Figure 7.** Dependence on time and temperature of the maximum reciprocal distance,  $s$ , and intensity at peak maximum of the first order diffraction of a sample heated from 20 to 40 °C at a rate of 1 °C/min and left to stabilize for 60 min at 40 °C constant temperature (O). Once 40 °C is attained, there is an initial relatively fast accommodation of the system that takes about 20 min after which the stacking distance continues to increase regularly, without an obvious asymptotic behavior in the time sampled. The intensity at the maximum ( $\Delta$ ) also increases indicating a sharpening of the peak with time. Notice that the  $s$  scale is unusually expanded.

decrease of its thickness with temperature. A similar trend is observed for the isobaric thermal expansion of alkanes<sup>41</sup> that the authors explain as follows: at low temperature, in our case below 40–45 °C, the chains behave like hard spheres, and the trans–gauche isomerization forces an increase of the specific volume; above this temperature, the number of voids already present in the system is enough to accommodate the chain conformation changes, reducing the importance of this parcel in the thermal expansion of the liquid. The reasoning presented by Troncoso et al.,<sup>41</sup> based on careful measurements and molecular simulation, should also apply to the case of the lateral thermal expansion of planar bilayers. However, it can not be excluded that the values of  $\sigma$  obtained by us for the region of low temperatures may be influenced by the asymmetry of the LUVET bilayer caused by the excessive curvature of the small radius vesicles that result from an area of the internal leaflet, approximately 18% inferior to that of the external one. The increase in  $R_H$  above 55 °C is probably a consequence of the shape of the vesicles diverging too much from a sphere. In this higher temperature region, the geometrical shape of the unilamellar vesicles may suffer drastic changes acquiring morphologies that result in a slower diffusion and enhance light dispersion.<sup>42,43</sup>

The results from the same experiment done with POPC LUVET are identical, with the same trend of  $R_H$  variation with temperature, the only difference being that the hydrodynamic radius of the vesicles varies between 49.9 nm at 20 °C and 53.0 nm at 70 °C.

#### Further Comments on the Experimental Observations.

For the MLV prepared at room temperature, there is no indication of irregularity of stacking until 40 °C, but this does not mean that the samples heated at 1 °C/min are at equilibrium. Our purely geometrical calculation based on the thermal expansion of the bilayers would predict a repeat distance smaller than that experimentally obtained. The DLS experiments, while prone to error, confirm that the value  $\sigma \approx 3.7 \times 10^{-3} \text{ K}^{-1}$  is too large as an average of the area thermal expansion of a DOPC bilayer in the 20 to 40 °C region, so it seems that the distance is forced to

smaller than equilibrium values by the external layers of the MLV. In Figure 7, the evolution with time of the maximum of the first order diffraction of a sample heated from 20 to 40 °C and kept at this temperature along one hour shows that after this relatively long time the repeat distance is still slowly increasing, indicating that the system is not at equilibrium. The change in distance at this slow rate may result from the exchange of DOPC between adjacent bilayers to reduce the compression/expansion to which the inner/outer bilayers are subjected or a readjustment of the several layers to attain a compromise between the possible and the equilibrium distance and tension. Along this stabilization time, it is also evident that the spatial correlation of the layers is improving because, as also shown in Figure 7, the peak is becoming sharper and its maximum increasing.

Above 40 °C, the MLV made and kept at room temperature and heated at 1 °C/min develop an irregular stacking of the bilayers with shoulders appearing in the diffractograms that eventually give origin to relatively sharp peaks at high temperature. If the heating is stopped and the sample maintained at a constant high temperature, these extra diffractions convert to the one at smaller  $s$  within about 40 min. The system evolves in this time range toward a pseudoequilibrium state with larger repeat distance that subsequently progress slowly for even larger distance, eventually to that found in the equilibrated samples, Figures 4 and 7. What remains to be understood is why, instead of a broad tail spreading to the region of large  $s$  values, some smaller than equilibrium distances are favored. The pattern of these multiple reflections is strongly dependent on the method of sample preparation, but whatever the method the final pseudoequilibrium attained is identical. Since the observed rearrangement is too fast to result from lipid migration, we suppose that the origin of these transient reflections is MLV populations that differ in the behavior to water permeation. In other words, there are MLV that react faster to the temperature, probably because they have fewer and/or more curved bilayers for which water permeation is easier, and others that being bigger and constituted by a larger number of bilayers take more time to adapt to the new geometry. The observation of a similar pattern with MLV-REV does not invalidate this explanation since the DLS of reverse phase vesicles shows discrete populations of distinct sizes that may originate the same result.

The appearance of nonidentical stacking distances only above 40 °C may be the consequence of the smaller bilayer–bilayer interaction energy at high temperature that, given enough time, will progress to a shape and distance that is a trade-off between the bilayer–bilayer interaction energy, bending energy, compression, and geometrical constraints. Experiments with oriented multilamellar stacks of POPC bilayers deposited on silicon in excess water<sup>44</sup> indicate that between 76 and 80 °C, the repulsive forces overcome the van der Waals attraction originating the so-called unbinding transition. Following this interpretation, above this temperature, no preferred distance should exist between two contiguous bilayers, and even if the multilamellar vesicles maintain its physical integrity, a single broad band should be observed in SAXS, which is not in agreement with the observed results. However, it has also been commented that the observation of the unbinding in that short temperature range may result from the particularities of the preparation, namely, the interaction of the bilayer with the silicon substrate.<sup>7</sup> Other authors found that the unbinding transition is not a first order transition, being continuous with onset at 77 °C for DMPC<sup>7</sup> what seems in better accordance with our observations even if we do not notice a change of behavior at that temperature. It is also worthy to note

that the same authors conclude that above 40 to 50 °C, coinciding with the temperature above which the new peaks appear in our experiments, the Helfrich undulation becomes the dominating repulsive force between bilayers. The reduced bilayer–bilayer interactions result in a poorer stacking and in a smaller driving force to attain an optimized shape within the possible boundaries. However, we cannot forget that the encapsulation of the vesicles within each other in a MLV will not allow a separation of the bilayers unless the repulsion is strong enough to break the external layers.

## CONCLUSIONS

The usefulness of SAXS for the study of lipid systems, namely, that of the lipid bilayers arranged in multilamellar vesicular structures, is partially compromised by its slow adaptation to thermal conditions different from those at which the MLV were prepared. The experiments presented clearly show that the only way to be absolutely sure that the system is in perfect equilibrium is to prepare and maintain the samples at the temperature at which the measurement is intended to be done.

This quite undesirable protocol can be partially circumvented by waiting enough time for equalizing the interbilayer spacing, ensuring that a stable single peak is obtained. This so-called enough time depends on the measurement temperature and has to be determined for each case. However, we have shown that after this thermal equilibration, the sample will not be in its lowest thermodynamic state, and the Bragg reflection corresponding to the lamellar repeat distance will slowly shift to larger distances, but this drift is so slow that for most purposes, it will not undermine the validity of the results.

All glycerophospholipids tested, DOPC, POPC, and DPPC, in excess water present the same kind of behavior, which is not a consequence of the particular method of preparation of the MLV samples or of impurities of the lipid. It is also presents when MLV-REV are used, showing that it is not related to the particular morphology of the MLV.

The explanation that we propose for this behavior is based on the geometrical constraints imposed by the characteristics of this kind of multilayer assemblies, structures where the migration of lipids between contiguous bilayers is a process too slow to be effective in the time span of most measurement techniques in normal conditions. The consequence is that, besides the force-balance between attraction and repulsion and the structural thermal oscillations that influence the average equilibrium distance between the membrane interfaces, there are also geometrical limitations created by the thermal expansion of the individual vesicles that force the distance between layers to values that are not necessarily those of minimum free energy.

Because of the identical thermal expansion of all concentric lamellae of the MLV and in the absence of lipid migration, it is inevitable that the interbilayer spacing eventually differs from the thermodynamic equilibrium interbilayer distance. From the experiments with DOPC, it seems that a uniform interbilayer distance is attained in a time that may vary between approximately 30 min and 2 h. It is also clear from the experiments that this uniform distance is not necessarily the equilibrium distance, which for DOPC is significantly larger.

## AUTHOR INFORMATION

### Corresponding Author

\*E-mail: eurico@itqb.unl.pt.

## ACKNOWLEDGMENT

This work was financially supported by FCT, Fundação para a Ciência e Tecnologia, Portugal, through contracts PTDC/QUI/68242/2006 and PTDC/SAU-FCT/69072/2006, and by HASYLAB of DESY, Germany, with project II-20060163 EC. H.L. and J.V. are indebted to FCT, Portugal, for grants BD/13765/2003 and 030/BI–BI/2009, respectively.

## REFERENCES

- (1) Huang, J. Y.; Buboltz, J. T.; Feigenson, G. W. *Biochim. Biophys. Acta* **1999**, *1417*, 89–100.
- (2) Rand, R. P.; Parsegian, V. A. *Biochim. Biophys. Acta* **1989**, *988*, 351–376.
- (3) Helfrich, W. *J. Phys.* **1985**, *46*, 1263–1268.
- (4) Servuss, R. M.; Helfrich, W. Forces and the Cohesion Energy of Egg-Lecithin Membranes. In *Physics of Complex and Supramolecular Fluids*; Safran, S. A., Clark, N. A., Eds.; Wiley: New York, 1987.
- (5) Servuss, R. M.; Helfrich, W. *J. Phys.* **1989**, *50*, 809–827.
- (6) Zhang, R. T.; Tristram-Nagle, S.; Sun, W. J.; Headrick, R. L.; Irving, T. C.; Suter, R. M.; Nagle, J. F. *Biophys. J.* **1996**, *70*, 349–357.
- (7) Gordeliy, V. I.; Cherezov, V.; Teixeira, J. *Phys. Rev. E* **2005**, *72*, 061913–1–061913–16.
- (8) Rappolt, M.; Pressl, K.; Pabst, G.; Laggner, P. *Biochim. Biophys. Acta* **1998**, *1372*, 389–393.
- (9) Rappolt, M.; Pabst, G.; Amenitsch, H.; Laggner, P. *Colloids Surf. A* **2001**, *183*, 171–181.
- (10) Pabst, G.; Hodzic, A.; Strancar, J.; Danner, S.; Rappolt, M.; Laggner, P. *Biophys. J.* **2007**, *93*, 2688–2696.
- (11) Sturtevant, J. M. *Annu. Rev. Phys. Chem.* **1987**, *38*, 463–488.
- (12) Estronca, L. M. B. B.; Moreno, M. J.; Vaz, W. L. C. *Biophys. J.* **2007**, *93*, 4244–4253.
- (13) Brewster, R.; Pincus, P. A.; Safran, S. A. *Biophys. J.* **2009**, *97*, 1087–1094.
- (14) Brewster, R.; Safran, S. A. *Biophys. J.* **2010**, *98*, L21–L23.
- (15) Pidgeon, C.; Hunt, A. H.; Ditttrich, K. *Pharm. Res.* **1986**, *3*, 23–34.
- (16) Pidgeon, C.; Mcneely, S.; Schmidt, T.; Johnson, J. E. *Biochemistry* **1987**, *26*, 17–29.
- (17) Dasler, W.; Bauer, C. D. *Ind. Eng. Chem.* **1946**, *18*, 52–54.
- (18) Bangham, A. D.; Standish, M. M.; Watkins, J. D. *J. Mol. Biol.* **1965**, *13*, 238–251.
- (19) Szoka, F.; Olson, F.; Heath, T.; Vail, W.; Mayhew, E.; Papahadjopoulos, D. *Biochim. Biophys. Acta* **1980**, *601*, 559–571.
- (20) Mayer, L. D.; Hope, M. J.; Cullis, P. R. *Biochim. Biophys. Acta* **1986**, *858*, 161–168.
- (21) Funari, S. S.; Barcelo, F.; Escriba, P. V. *J. Lipid Res.* **2003**, *44*, 567–575.
- (22) Szoka, F.; Papahadjopoulos, D. *Proc. Natl. Acad. Sci. U.S.A.* **1978**, *75*, 4194–4198.
- (23) Burchard, W. Combined Static and Dynamic Light Scattering. In *Light Scattering. Principles and Development*; Brown, W., Ed.; Clarendon Press: Oxford, U.K., 1996.
- (24) Tristram-Nagle, S.; Nagle, J. F. *Chem. Phys. Lipids* **2004**, *127*, 3–14.
- (25) Costigan, S. C.; Booth, P. J.; Templer, R. H. *Biochim. Biophys. Acta* **2000**, *1468*, 41–54.
- (26) Pan, J.; Tristram-Nagle, S.; Kucerka, N.; Nagle, J. F. *Biophys. J.* **2008**, *94*, 117–124.
- (27) Safinya, C. R.; Roux, D.; Smith, G. S.; Sinha, S. K.; Dimon, P.; Clark, N. A.; Bellocq, A. M. *Phys. Rev. Lett.* **1986**, *57*, 2718–2721.
- (28) Roux, D.; Safinya, C. R. *J. Phys. (Paris)* **1988**, *49*, 307–318.
- (29) Zhang, R. T.; Sun, W. J.; Tristram-Nagle, S.; Headrick, R. L.; Suter, R. M.; Nagle, J. F. *Phys. Rev. Lett.* **1995**, *74*, 2832–2835.
- (30) Laggner, P.; Kriechbaum, M.; Rapp, G. *Chem. Phys. Lipids* **1991**, *57*, 121–145.

- (31) Tenchov, B.; Koynova, R.; Rappolt, M.; Rapp, G. *Biochim. Biophys. Acta* **1999**, *1417*, 183–190.
- (32) Israelachvili, J. N.; Mitchell, D. J.; Ninham, B. W. *Biochim. Biophys. Acta* **1977**, *470*, 185–201.
- (33) Nagle, J. F.; Tristram-Nagle, S. *Biochim. Biophys. Acta* **2000**, *1469*, 159–195.
- (34) Jones, J. D.; Thompson, T. E. *Biochemistry* **1989**, *28*, 129–134.
- (35) Abreu, M. S. C.; Moreno, M. J.; Vaz, W. L. C. *Biophys. J.* **2004**, *87*, 353–365.
- (36) Huster, D.; Jin, A. J.; Arnold, K.; Gawrisch, K. *Biophys. J.* **1997**, *73*, 855–864.
- (37) Mathai, J. C.; Tristram-Nagle, S.; Nagle, J. F.; Zeidel, M. L. *J. Gen. Physiol.* **2008**, *131*, 69–76.
- (38) Evans, E.; Needham, D. *J. Phys. Chem.* **1987**, *91*, 4219–4228.
- (39) Kojro, Z.; Lin, S. Q.; Grell, E.; Ruf, H. *Biochim. Biophys. Acta* **1989**, *985*, 1–8.
- (40) Brocca, P.; Cantu, L.; Corti, M.; Del Favero, E.; Motta, S. *Langmuir* **2004**, *20*, 2141–2148.
- (41) Troncoso, J.; Navia, P.; Romani, L.; Bessieres, D.; Lafitte, T. *J. Chem. Phys.* **2011**, *134*, 094502–1–094502–11.
- (42) Julicher, F.; Seifert, U.; Lipowsky, R. *Phys. Rev. Lett.* **1993**, *71*, 452–455.
- (43) Linke, G. T.; Lipowsky, R.; Gruhn, T. *Phys. Rev. E* **2005**, *71*, 051602–1–051602–7.
- (44) Vogel, M.; Munster, C.; Fenzl, W.; Salditt, T. *Phys. Rev. Lett.* **2000**, *84*, 390–393.